sustainability

MDPI

Article

The Characteristics of Rainfall-Runoff Generation and Its Influencing Factors in a Desert Steppe, China

Hasituya [1], Jiahong Liu [2,*] and Tiejun Liu [3,*]

[1] College of Grassland, Resources and Environment, Inner Mongolia Agricultural University, No. 29, Ordos East Street, Hohhot 010011, China; hasituya@imau.edu.cn
[2] State Key Laboratory of Simulation and Regulation of Water Cycle in River Basin, China Institute of Water Resources and Hydropower Research, No. 1, Fuxing Road, Beijing 100038, China
[3] Institute of Pastoral Water Resources, Ministry of Water Resources, No. 128, University East Street, Hohhot 010020, China
* Correspondence: liujh@iwhr.com (J.L.); mksltj@126.com (T.L.)

Abstract: Understanding the effect of land surface characteristics on rainfall-runoff generation is crucial in mastering the mechanisms of soil and water conservation. To characterize rainfall-runoff generation in desert steppes and to quantify the contribution of different influencing factors, a field-simulated experiment with three land degradation levels and three rainfall intensities (RIs) was conducted in the Inner Mongolia Desert Steppe. The results revealed that rainfall-runoff generation in different degraded plots at various RIs differed significantly. The runoff was generated faster and accumulated larger volumes under high RIs and heavy degradation levels (HDs) in comparison with generation under moderate/light degradation levels (MDs/LDs) and moderate/low RIs. The accumulated runoff over 40 min under a high RI on the HD plot is 153.37 L, which is much larger (0.77 L) than that under a low RI on the LD plot. The result from the structural equation model (SEM) indicated that RI is the most important factor directly driving rainfall-runoff generation, and its standardized path coefficient reached a value of 0.52. The vegetation condition is the second direct factor, with a standardized path coefficient of −0.51. However, the soil water content (SWC) has an indirect impact on rainfall-runoff generation through affecting vegetation conditions. So, interactions also exist between variables such as vegetation and soil. Therefore, the rainfall-runoff generation in the desert steppe may be mitigated through an enhancement of the vegetation and soil properties or through optimizing the interaction relationship between soil and vegetation.

Keywords: rainfall simulation; runoff generation; influencing factors; structural equation model

check for updates

Citation: Hasituya; Liu, J.; Liu, T. The Characteristics of Rainfall-Runoff Generation and Its Influencing Factors in a Desert Steppe, China. *Sustainability* **2023**, *15*, 15531. https://doi.org/10.3390/su152115531

Academic Editor: Jan Hopmans

Received: 6 September 2023
Revised: 19 October 2023
Accepted: 20 October 2023
Published: 1 November 2023

Copyright: © 2023 by the authors. Licensee MDPI, Basel, Switzerland. This article is an open access article distributed under the terms and conditions of the Creative Commons Attribution (CC BY) license (https://creativecommons.org/licenses/by/4.0/).

1. Introduction

Understanding the rainfall-runoff processes and their influencing factors is a very complex task. The factors influencing rainfall-runoff generation can be roughly divided into two classes: watershed characteristics and rainfall characteristics. Watershed characteristics include topographies, soil properties, land uses, and land covers [1]. Rainfall characteristics include rainfall intensity (RI), velocity, duration, direction, and temporal distribution [2]. Among the rainfall characteristics, the RI and rainfall duration are the two most dominant factors in hydrological processes. The relationships between rainfall and runoff often present large spatial and temporal variations due to the complex interactions between the controlling parameters. In particular, the land cover at the watershed scale is undergoing unprecedented changes that directly affect the rainfall-runoff generation process [3,4].

Presently, grassland degradation, including the degradation of soil, vegetation, water, and ecosystem function, has become a severe ecological problem. Grassland degradation has a serious impact on the production and development of animal husbandry and threatens the ecological environment's quality and security, ultimately bringing risk to the health of the soil–plant–air system.

The desert steppe in Inner Mongolia is an extremely fragile ecosystem and is currently undergoing severe degradation, such as the reduction in vegetation coverage (VC), vegetation height (VH), aboveground biomass (AB), plant diversity, and productivity due to natural (warming, drying) and human-made disturbances (grazing, mining). Influenced by land degradation, surface runoff and runoff erosion are becoming more and more serious and are susceptible to the rainfall characteristics (size and energy of raindrops and the spatial–temporal distribution) in this region.

Evidently, an understanding of understanding rainfall-runoff generation characteristics is essential for soil and water conservation, water resource management, and hydrological modeling. Therefore, the impact of land cover degradation on the rainfall-runoff generation process and the response of rainfall-runoff generation to land cover degradation have become an urgent concern in the field of ecohydrology [5–8]. In order to capture rainfall-runoff generation characteristics, many studies with diverse field or laboratory setups at various spatial scales have been carried out in the past. The results pointed out that the overall heterogeneity within a watershed has a significant impact on runoff generation patterns [1,9,10]. Several plot-scale rainfall simulation experiments have been carried out to explore rainfall-runoff generation characteristics and to determine the effect of antecedent soil water content (SWC) conditions, VC, and the spatial–temporal scale on rainfall-runoff generation [11,12]. These studies show that plot-scale rainfall-runoff experiments are a basic, effective, and popular approach for investigating and characterizing rainfall-runoff generation and its influencing factors in different ecosystems [13–15]. Studies have also revealed that surface runoff generation is closely related to the infiltration capacity of soil and land cover changes [10,16,17]. In particular, VC, distribution pattern (DP), and plant diversity (PD) have significant influences on runoff generation [18–21]. Some other studies have also revealed that uncertainties in rainfall data can be translated into uncertainties in runoff predictions [22]. As we can imagine, it is challenging to observe the rainfall-runoff generation process regularly under natural rainfall conditions due to difficulties in controlling rainfall intensity and duration. Furthermore, on-site rainfall simulation experiments can not only reflect natural scenarios as closely as possible, but the rainfall parameters (e.g., RI and rainfall duration) can also be controlled and the testing period can be shortened. Then, the instability and unpredictable variability of natural rainfall can be reduced as much as possible [23]. Due to the repeatability of rainfall event data, enabled by rainfall simulators, we can characterize rainfall-runoff generation patterns and evaluate the influencing factors more objectively [24]. Accordingly, rainfall simulation has been widely used as an effective approach for predicting surface runoff in various systems [25].

Several notable studies have been carried out in recent years from the perspective of exploring the effect of different influencing factors. For example, studies have been carried out which examine the effects of topography [26], soil hydrophobicity and antecedent soil moisture [27,28], rainfall intensity, and land use patterns on runoff generation [29,30]. There are also studies that have focused on the effect of drought and vegetation restoration on runoff generation processes [31–33]. All these studies were devoted to indicating that the environmental factors influencing runoff vary among different ecosystems.

However, an explanation of the effects of different degradation levels and rainfall intensities on runoff generation in desert steppes is not presently available. The responses of hydrological process to vegetation degradation in desert steppes remain unclear. Due to desert-steppe-specific geological and climatological conditions, the mechanisms that generate runoff in desert steppes may differ from other land use types or other grassland types. Furthermore, various factors control runoff generation, and their interactions are complicated. Thus, it is important to explore rainfall-runoff generation characteristics and identify the dominant factors controlling runoff generation in desert steppes with different degradation levels to assist in managing ecological and hydrological processes, grassland restoration, and soil and water conservation.

In the present study, we hypothesized that there is a hydrological consistency in rainfall-runoff generation characteristics (e.g., same volume of runoff) under the same surface condition, i.e., if the land surface condition is changed, then the rainfall-runoff generation characteristics change accordingly. We designed artificial rainfall simulation experiments with three RIs and three different degradation levels in a desert steppe for the following reasons: (1) to identify the main characteristics of the rainfall-runoff generation in the desert steppe; (2) to quantify the contribution of various factors to rainfall-runoff generation and to determine which factors are the most important factors. This study is expected to provide a scientific reference for water resource management and soil and water conservation from the perspective of a fragile grassland ecosystem and to provide a basis for developing hydrological models to reveal the laws of hydrological cycles at larger scales.

2. Materials and Methods

2.1. Study Region

The study area (Figure 1) is located in Shangdong River watershed (41°12′–41°31′ N, 111°00′–111°20′ E, covering an area of 720 km^2), a tributary of the inland Tabu River, Xilamuren Desert Steppe, Inner Mongolia Autonomous Region. This area has a mid-temperate semi-arid continental monsoon climate with long and cold winter, short and hot summer, large disparities between day and night temperatures, little and unevenly distributed precipitation and large evaporation (2305 mm), a short frost-free period (83 days), and high cumulative temperatures. The annual average precipitation is 282.4 mm and is mainly concentrated in June, July, and August. Following several years of investigation and testing, we have determined that the main plant species in this region include *Stipakrylovii Roshev*, *Stipa breviflora Griseb*, *Leymus chinensis*, *Agropyron cristatum*, *Artemisia frigida Willd*, and *Convolvulus ammannii Desr*, and the main soil texture in this region includes sandy loam and light loam. The main soil types include chestnut soil and brown calcium soil.

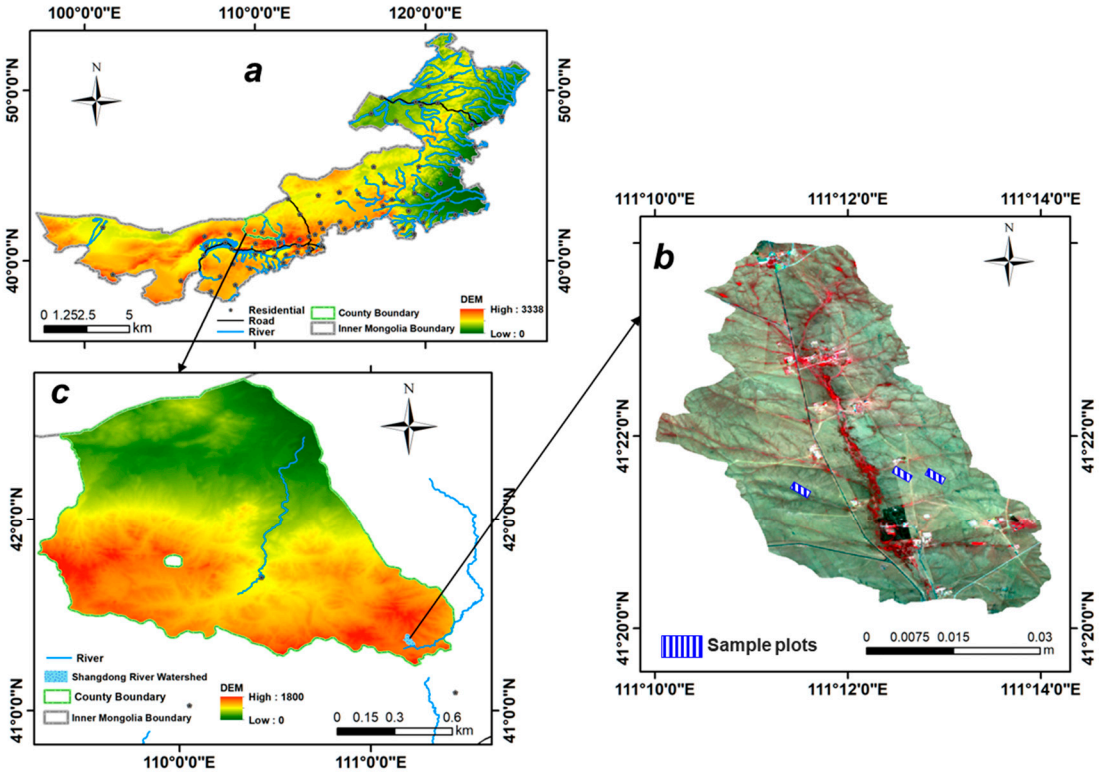

Figure 1. Location of the experiment region ((**a**) boundary of Inner Mongolia Autonomous Region; (**b**) experiment site; the image in (**b**) is the standard false color composite Sentinel-2 image; (**c**) boundary of Darhan Maoming'an United Banner).

2.2. Experimental Design

2.2.1. Selection and Design of Sample Plot

Considering the representativeness of samples and the feasibility of conducting experiments, the sample plots were set at the middle–lower part southern part of the slope. At the top of the slope, it would be more difficult to conduct the experiments; additionally, at the upper part, it is hard to find a flat sample region. Meanwhile, at the bottom of the slope, there may be water accumulation from precipitation or rivers, which will affect the rainfall-runoff characteristics. So, the middle part is a more suitable area for conducting the artificial rainfall experiment in this study.

The different degradation levels were determined through an on-site expert's judgment in combination with information from the National Standards of grassland degradation, China (GB+19377-2003) [34]. According to the dominant species of community, vegetation coverage, above-ground biomass, and the surface soil properties (Table 1), especially the indicator species, we designed three degradation levels for observing the rainfall-runoff generation characteristics: lightly degraded plots (LD), moderately degraded plots (MD), and heavily degraded plots (HD). The field investigation and experiment were carried out during 13–20 July 2017.

Table 1. The standard of grassland degradation levels.

Indexes	Lightly Degraded Plots (LD)	Moderately Degraded Plots (MD)	Heavily Degraded Plots (HD)
Dominant species of community	*Stipa breviflora*, *Stipa kleinii*	*Artemisia frigida*	*Convolvulus argentatus*
Vegetation coverage (%)	30–35	20–30	<20
Aboveground biomass (g/m^2)	60–80	35–50	<35
Surface soil properties	more fine particles, high organic matter	desertification, low organic matter	desertification, coarsening, low organic matter

2.2.2. Design of the Rainfall Simulation

The development of rainfall simulators has accelerated recently both domestically and internationally. Rainfall simulators can be divided into four types: suspension, needle, pipe network, and sprinkler. The raindrops produced by suspension- and needle-type rainfall simulators are uniform in size, while the pipe-network- and sprinkler-nozzle-type rainfall simulators can spray with a given initial rate through changing the water pressure; the raindrop size and RIs of such simulators can be controlled through adjusting the working frequency of the water pump. These kinds of simulators can meet the testing requirements easily and can effectively simulate real-world rainfall conditions. Thus, a sprinkler-type system was used to simulate rainfall. It was composed of eight nozzle groups; and each group of nozzles comprised three independent solenoid valve nozzles with differently sized apertures. The desired RIs and raindrop sizes for each group were produced through controlling the number of active nozzles. Photos of the rainfall simulation device are shown in Figure 2.

The effective rainfall area of the simulated rainfall device was 3 m × 5 m; the height of the nozzles was 4 m above the ground surface. RI was determined according to the average rainfall for the past ten years (Figure 3). The highest level of rainfall in the past ten years did not exceed 60 mm/h. Therefore, the RIs were designed at three levels, 20, 40, and 60 mm/h, and these were implemented in plots with different degradation levels.



Figure 2. Photos of the rainfall simulation device: (**a**) installation of the rainfall simulation; (**b**) equipment for controlling rainfall intensity.

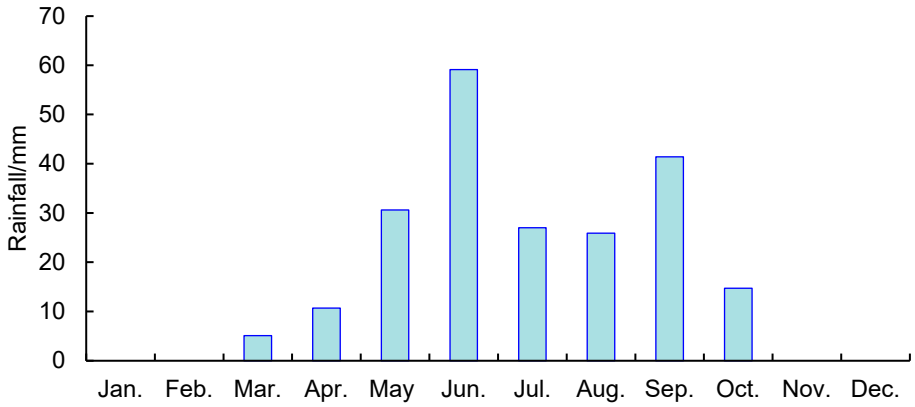

Figure 3. The temporal distribution of rainfall in this study region.

2.2.3. Design of the Runoff Experiment

The rainfall simulators were installed at three sample plots with different degradations. The perimeter walls around the plots were constructed using clay bricks and cement mortar (Figure 4). The height of the walls was 50 cm: 30 cm of the wall was below the ground surface and 20 cm was above the ground surface. An underground pipe with a 15 cm diameter was installed in the middle of the perimeter wall at the end of each plot. These pipes introduce runoff into the collecting tanks. The internal wall of the collecting pool (80 cm × 80 cm × 80 cm) was 50 cm away from the bottom of the runoff area. It was made of cast-in-place reinforced concrete. The properties of the runoff plot are presented in Table 2.

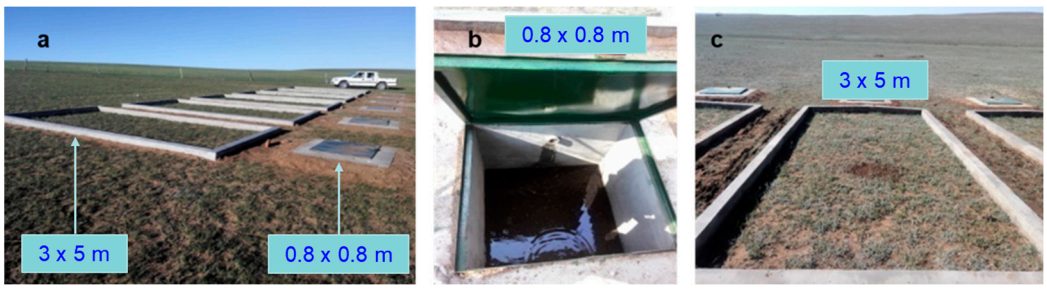

Figure 4. Field photo of the experimental runoff setups: (**a**) overview of runoff subplots; (**b**) photo of a runoff collection tank; (**c**) photo of a single runoff subplot.

Table 2. Properties of different rainfall-runoff plots.

ID	Length	Width	Slope	Degradation	Soil Physical Properties							
					Initial Water Content (%)				Bulk Density (g/m^3)			
					0–5 cm	5–10 cm	10–15 Cm	15–20 cm	0–5 cm	5–10 cm	10–15 cm	15–20 cm
1	5 m	3 m	2.80°	LD	4.0	3.8	4.4	4.3	1.40	1.45	1.40	1.45
2	5 m	3 m	2.78°	MD	5.0	4.8	3.9	5.4	1.49	1.56	1.49	1.41
3	5 m	3 m	2.81°	HD	2.9	2.9	3.5	5.3	1.38	1.38	1.33	1.46

2.2.4. Measurement of Each Parameter

- Rainfall value determination:

The amount and intensity of rainfall are the most important parameters for generating runoff. We designed the different RI levels and implemented the rainfall simulation experiment through the use of an RI controller. We calibrated the rainfall simulator through controlling the water pump to ensure a stable rainfall intensity and ensured the accuracy of rainfall intensity by $\pm$ 0.05. The rainfall volume was obtained through the multiplication of RI, the duration time, and the plot area. Generally, the rainfall values were 225 L, 350 L, and 375 L for HD, 275 L, 400 L, and 450 L for MD, and 300 L, 450 L, and 525 L for LD under RIs of 20, 40 and 60 mm/h, respectively.

- Runoff measurement:

A stopwatch was used to record the time of start and the end of each rainfall event and the runoff generation. Three repeats were performed for each RI. The runoff was collected manually. When the runoff volume was small, a 50 mL graduated cylinder was used to collect the runoff for one minute at intervals of two minutes. When the runoff volume was large, a 1000 mL graduated cylinder was used to collect the runoff, and the volume collected in the graduated cylinder was recorded once every five minutes. Each event was terminated when the collected runoff was approximately consistent over three consecutive events; finally, the total runoff in the collecting tank was measured to an accuracy of 0.01 L. When the runoff reached its peak, the timing and volume were recorded; then, as the runoff decreased, the timings and volumes of runoff were recorded three more times for each event. However, because of the large disparity in the morning and afternoon microclimates in the study region, we only observed the delayed runoff volume and did not observe their duration time, to ensure consistency in climatic conditions and shorten the testing time. Thus, this component of the delayed runoff characteristics was not considered in our analysis.

- The vegetation investigation:

To evaluate the effects of vegetation, three indicators (VC, VH, and AB) were selected in this study. The vegetation investigation was conducted in mid-August. Samples measuring 1 $\times$ 1 m with three repeats in each degraded plot were designed and surveyed. Through an identification by several experts, we found that the plant species in different degradation plots were different. In general, plant species included *Stipa breviflora*, *Stipa kleinii*, *Artemisia frigida*, *Cryptocarpa*, *Convolvulus argentatus*, etc. The VC was measured using the projection method and through a calculation of the ratio of the covered area to the sample area. VH was measured using a ruler, and the average height of 10 plants was recorded. AB was measured using the mowing method. The AB samples were placed in a sample bag and separately indexed after mowing; they were brought back to the laboratory and dried at 80 °C until they reached a constant weight. The measured accuracies of VC, VH, and AB were controlled to 1 cm, 1%, and 0.1 g/m^2, respectively.

- Soil water content measurement:

The SWC was tested using a soil moisture sensor, EC-5, manufactured by Meter Group Inc., Pullman, WA, United Sates. The measurement accuracy reached $\pm$1%$-$2% of the

volume moisture content. EC-5 sensors were installed in the middle of each runoff plot after calibration. The buried depths were 5 cm, 10 cm, 15 cm, and 20 cm, which correspond with the SWCs with soil layers of 0–5 cm, 5–10 cm, 10–15 cm, and 15–20 cm, respectively. The time interval of collection was set to 1 min. The EC-5 was connected with the external data collector EM50 for automatic data collection.

However, the change in surface SWC after natural rainfall will impact the infiltration and runoff generation; then, it significantly impacts the results of the rainfall-runoff simulation experiment. In order to minimize the influence of natural rainfall on SWC, we selected a sunny day, after no natural rainfall had occurred for one continuous week. The 0–5 cm SWC is relatively close to the surface SWC following one week of no rainfall, which can ensure that the influence of soil moisture on the simulated rainfall experiment was reduced to a great extent. The rainfall simulation experiment was conducted in late July–early August, because both the annual rainfall frequency and amount tend to decline during this time.

- Soil bulk density measurement:

A ring knife (cylindrical metal soil picker) with a certain volume (usually 100 cm^3) was inserted into the soil to collect soil samples, and the dry soil weight was obtained after drying (105–110 °C, 24 h). Soil bulk density (SBD) was calculated through a computation of the dry soil mass per unit volume.

- Soil texture:

In this experiment, we did not determine the soil texture through soil sampling or soil tests. Soil texture was determined in a previous experiment through a hydrometer method in the laboratory; the obtained results indicated that silty loam is the main soil texture in this region. The characteristics of silty loam soil texture are moderate permeability and poor water stability. Once soil water reaches a saturation level, soil erosion occurs easily.

In addition, we considered the influence of wind. In our experimental region, the wind in the afternoon is much stronger than that in the morning, which has a huge impact on the effectiveness of the simulated rainfall experiment. In order to avoid errors caused by changes in wind between the morning and afternoon, the experiment was carried out in the morning.

2.2.5. Data Analysis

- Regression analysis

The runoff coefficient (RC) is a significant indicator describing hydrological processes [35]. RC is defined as the ratio of total runoff to precipitation over a period of time in a certain watershed area. RC is calculated using the following equation [9]:

$$RC = \frac{R_d}{P} \quad (1)$$

where R_d is the runoff depth (mm) and P is the rainfall volume (mm). The event RC is defined as the fraction of rainfall converted to direct or quick runoff during an event [36]. RC provides basic information on the effects that climate and watershed characteristics have on the runoff generation [37]. The runoff depth is calculated using the following equation [38].

$$R_d = \frac{R_c}{A_p} \quad (2)$$

where R_d is the runoff depth (mm) of each plot, R_c is the cumulated runoff volume in each plot, and A_p is the area of plots.

- Principal component analysis (PCA)

Principal component analysis (PCA) is a multivariate statistical method to investigate the correlation between multiple variables, and often used to recombine many original

correlations into a new set of independent comprehensive indicators to replace the original indicators [39]. PCA can derive a few principal components from the original variables and make them keep as much information of the original variables as possible. In this study, PCA was used to determine the total explanatory of the selected factors influencing the rainfall-runoff generation. The factoextra 1.0.7 package in R 4.3.1 was used to carry out PCA.

- Structural Equation Model

Structural equation modeling (SEM) is a widely used approach for establishing, estimating, and testing causal relationship models. SEM is an extension of the multivariate regression model and can be used to test the fitness of multiple causal relationships and to identify the effect of one variable on other variables [40,41]. The model contains not only measurable variables, but also latent variables that cannot be directly observed. SEM can clearly analyze the effect of individual indicators on the overall and the relationship between individual indicators.

The construction of SEM according to prior knowledge is not necessarily correct and perfect. It needs to be debugged and optimized. The maximum likelihood (ML) estimation method and the principles of "increase and decrease" were used to debug and estimate the constructed SEM in this study. The "Increase" principle functions through increasing the correlation between variables to improve the fitness of a model by selecting the path with a relatively higher MI value. If a path is added, then the chi-square value decreases and a fitting index is significantly increased, which indicates that the correlation is meaningful. The "Decrease" principle functions through deleting the variables with insignificant path coefficients. If there are multiple insignificant paths, then the least significant path is deleted first, and one should proceed with regression [42]. In this study, we developed and optimized an SEM to quantify the contribution of different factors to rainfall-runoff generation and to determine the interactions between factors; the results of the reliability analysis were also provided.

Our basic hypothesis was that the three subsystems (rainfall, vegetation, and soil) could affect rainfall-runoff generation either directly or indirectly through influencing each other. Therefore, according to the common knowledge of rainfall-runoff generation and the results from PCA, an SEM conceptual framework was constructed. A partial least squares structural equation model (PLS-SEM) was used to quantify the response of RC to the influencing factors. There was no error report when the theoretical model was established, based on the single direction influence theory; additionally, there were no hints of an influence of double direction when optimizing the model. Thus, it was treated as a single direction influence in the variables in our study. Multiple linear regression was applied to obtain the values of the latent variables through iterating the external and internal model estimations. Then, the path coefficients were calculated, and the PLS-SEM was constructed. The goodness-of-fit calculation (GOF > 0.60), Cronbach's alpha (>0.70), and DG.rhowas (>0.70) were used to determine the fitness of model for this application. The "PLSPM" package in R 4.4.2 was used to develop and operate the SEM.

3. Results

3.1. The Rainfall-Runoff Generation Characteristics in the Desert Steppe

The rainfall-runoff generation characteristics in the chosen desert steppe was were explained by using the starts start times of the runoff, the time taken until to stable runoff occurred, and the cumulative runoff in over 40 min.

Table 3 presents the rainfall-runoff generation characteristics in the LD, MD, and HD plots. In the LD plots, under RIs of 20 mm/h and 40 mm/h, the runoffs began 27′18″ and 22′5″ after rainfall, respectively, and the cumulative runoffs in 40′ was 0.77 L and 5.75 L, respectively. However, under the RI of 60 mm/h, the runoff started just 5′8″ after rainfall and the cumulative runoff in 40′ was up to 92.81 L. It took 60′, 45′, and 35′, respectively, to reach a stable trend for the RIs of 20 mm/h, 40 mm/h, and 60 mm/h; meanwhile, in the MD plots, runoffs began 17′2″ and 14′56″ after rainfall, and the cumulative runoffs in

40′ were 10.10 L and 10.99 L, respectively, under RIs of 20 mm/h and 40 mm/h. Under an RI of 60 mm/h, the runoff generated quickly (needing only 5′4″), and the cumulative runoff over 40′ was up to 137.20 L. However, in the HD plots, the runoffs occurred 14′59″, 13′17″, and 3′20″ after rainfall under RIs of 20 mm/h, 40 mm/h, and 60 mm/h, and their cumulative runoffs over 40′ were 16.66 L, 22.29 L, and 153.37 L, respectively. Therefore, for different degradation levels, the higher the RI was, the shorter the time that was required to generate runoff and to reach stable runoff, and the greater the cumulated runoff volume. At each RI level, the cumulative runoff volume in the different degraded plots showed a trend of LD < MD < HD; the start times of rainfall-runoff generation in different degraded plots were in the order of LD > MD > HD. This indicates that, in LD plots, the vegetation was well-developed, and both the surface roughness and the soil infiltration were high, so runoff generation required a longer time. In general, the RI and the degradation level have a synergistic effect on the rainfall–runoff generation.

Table 3. Characteristics of runoff pattern of plots with different degradation levels.

Plot Types	Rainfall Intensity (mm/h)	Start Time of Runoff (min:s)	Time Taken to Establish Stable Runoff (min)	Cumulative Runoff in 40 min (L)
LD	20	27′18″	60	0.77
	40	22′05″	45	5.75
	60	05′08″	35	92.81
MD	20	17′21″	55	10.10
	40	14′56″	40	10.99
	60	05′04″	30	137.20
HD	20	14′59″	45	16.66
	40	13′17″	35	22.29
	60	03′20″	25	153.37

In general, the increase in cumulative runoff over 40 min was 5–44 L when induced by the degradation level, and 0.8–131 L when induced by the RI. The reduction in the time taken to establish a stable runoff caused by the degradation level was 5–10 min, and that caused by the RI was 10–15 min. The largest advancement of the start time of the runoff was roughly 17 min when caused by the RI and 10 min when caused by the degradation level. Therefore, a larger range of changes in runoff generation was induced by the RI than by the degradation levels.

The characteristics of the rainfall-runoff generation in different degraded plots at various RIs are depicted in Figure 5. We can see that the characteristics of the rainfall-runoff generation in LD plots (Figure 5a–c) show gradual increasing trends at the start times; then, they increase sharply to approach stability under an RI of 20 mm/h. Meanwhile, under RIs of 40 and 60 mm/h, the runoff curves originated at the starting time of the rainfall and increased sharply to reach stable runoff levels, with a little fluctuation. The runoff generations in the MD plots (Figure 5d–f) were similar to those in the LD plots. The runoff curves exhibited gradually increasing trends at the beginning, followed by sharp increases, and finally became stable. However, there were clear dips which are likely attributable to slope runoff confluence and depression filling. When RI was 60 mm/h, the curve of the cumulative runoff revealed a rapid two-stage increase. However, the runoff generation in the HD plots fluctuated significantly (Figure 5g–i). In particular, the fluctuations in the runoff curves are most evident for an RI of 40 mm/h. This indicates that, when RI is low, soil infiltration is satisfactory, and runoff generation is slow. Under a high RI, soil infiltration is poor, so runoff generation is rapid and quickly stabilized. The main reason for this fluctuation may be the low level of plant cover and the thin topsoil layer of aeolian sand in the HD plots.

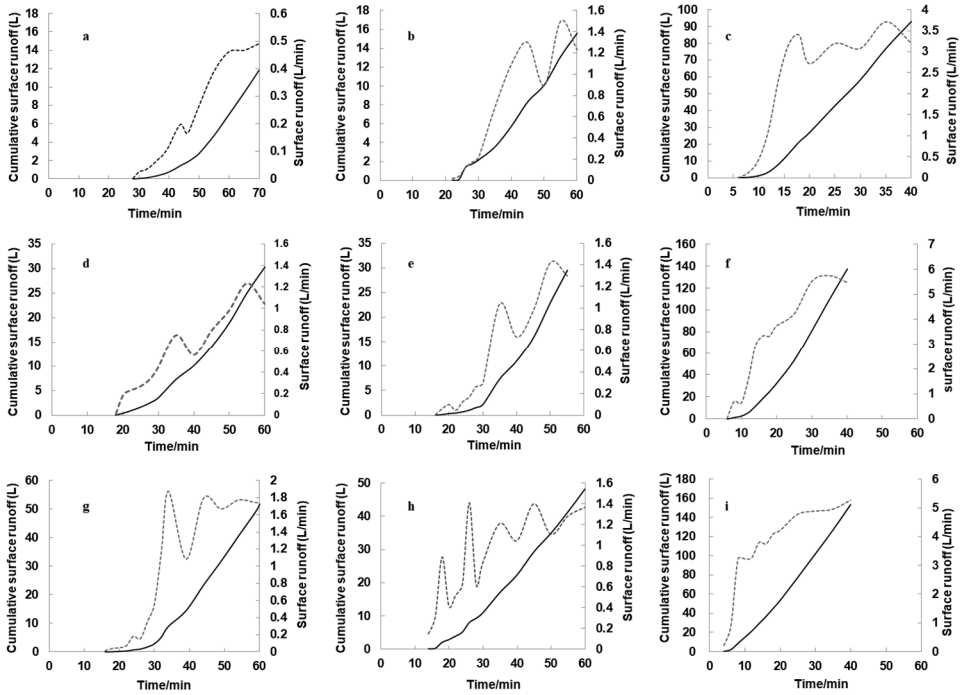

Figure 5. Rainfall-runoff generation in different degraded plots under different rainfall intensities (the dotted lines depict the surface runoff and the solid lines depict the cumulative surface runoff; (**a**–**c**) represent the rainfall-runoff generation in lightly degraded (LD) plots under the rainfall intensities of 20, 40, and 60 mm/h, respectively; (**d**–**f**) represent the rainfall-runoff generation in moderately degraded (MD) plots under the rainfall intensities of 20, 40, and 60 mm/h, respectively; (**g**–**i**) represent the rainfall-runoff generation in heavily degraded (HD) plots under rainfall intensities of 20, 40, and 60 mm/h, respectively).

3.2. Influencing Factors of Rainfall-Runoff Generation in Desert Steppe

To determine the influence of RI and vegetation conditions on rainfall-runoff generation in the chosen desert steppe, we calculated the RC for the period between the start of the rainfall and the timing of the maximum runoff to develop the relationship between RC and the influencing factors. The delayed runoff and its duration were not considered in the calculations of the RC due to difficulties encountered during the field experiment.

3.2.1. Influence of Rainfall Intensity on Runoff Generation

As shown in Figure 6, there was a significant linear positive correlation between RC and RI in the HD plots ($p < 0.05$), and a significant positive exponential function correlation was observed in the MD and LD plots ($p < 0.05$). This implies that RI had a significantly positive influence on the runoff coefficient in HD plots.

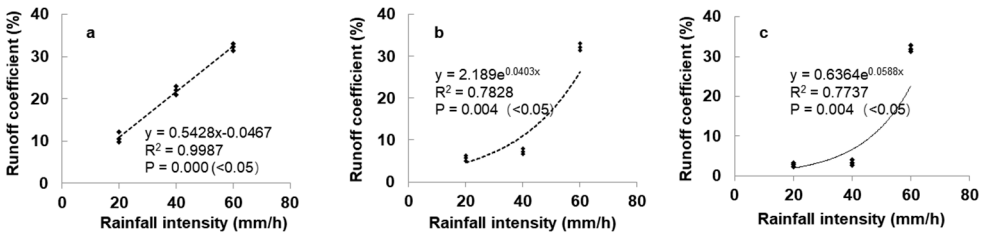

Figure 6. Relationships between runoff coefficients and rainfall intensities: (**a**–**c**) relationships in the HD, MD, and LD plots, respectively.

3.2.2. Influence of Vegetation Status on Runoff Generation

Figure 7 represents the relationships between RC and vegetation characteristics. RC had a significant negative linear correlation with AB in all three plots ($p < 0.05$) (Figure 7a–c), and RC levels were negatively correlated with VC in the three plots ($p < 0.05$) (Figure 7d–f). The increases in VC resulted in significant decreases in RC. The runoff coefficient decreases with increases in VC and AB in this region.

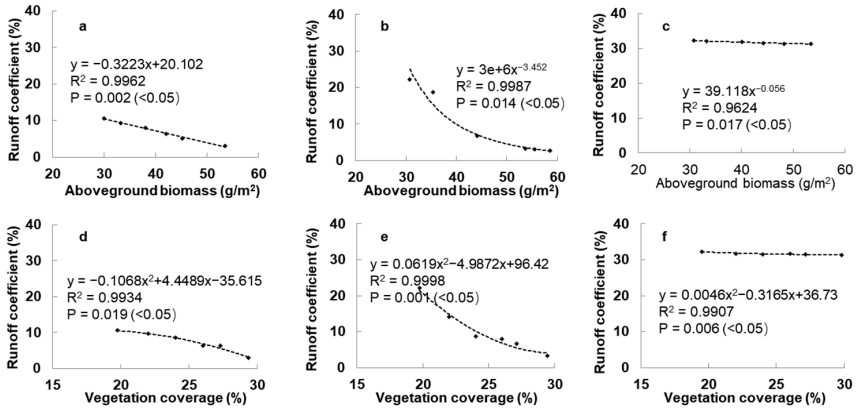

Figure 7. Relationships between runoff coefficients and vegetation characteristics ((**a**–**c**) relationships between RC and the aboveground biomass in the HD, MD, and LD plots, respectively; (**d**–**f**) relationships between RC and the vegetation coverage in the HD, MD, and LD plots, respectively).

3.3. Principal Component Analysis

PCA was used to facilitate the grouping of the factors which affected the rainfall-runoff generation, permitting an analysis of the overall explanation of the selected factors. From Figure 8, we can see that the selected influencing factors can explain 74.7% of the total runoff generation; PCA-1 can explain 52.5%; PCA-2 can explain 22.2% ($p < 0.05$). The difference between the LD and HD plots for runoff generation was mainly related to RI, VH, AB, and VC; the difference between the LD and MD plots and the difference between the HD and MD plots were related to SBD, SWC, VC, and AB.

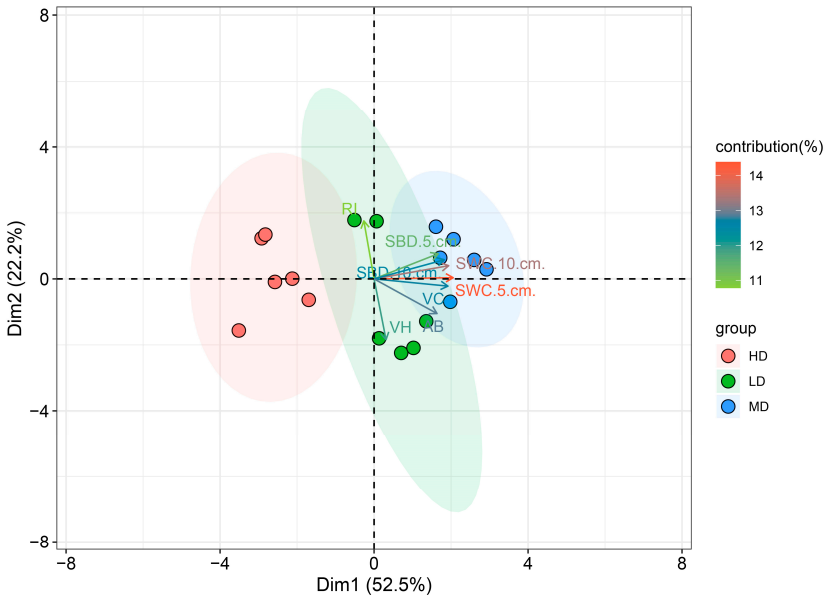

Figure 8. Principal component analysis of the relationships between rainfall, vegetation condition, and soil properties and runoff generation (HD, LD, and MD represent the three degradation levels and RI, RC, VC, AB, VH, SWC, and SBD represent the rainfall intensity, runoff coefficient, vegetation coverage, aboveground biomass, vegetation height, soil water content, and soil bulk density, respectively).

Figure 9 displays the contribution of each factor to PCA-1 and PCA-2. We can see that the 5 cm SWC layer has the biggest contribution (20.5%) to PCA-1, followed by the 10 cm SWC layer (18.2%) and VC (17.9%). And for PCA-2, the three top factors which contributed were VH (38.9%), RI (35.5%), and AB (12.7%).

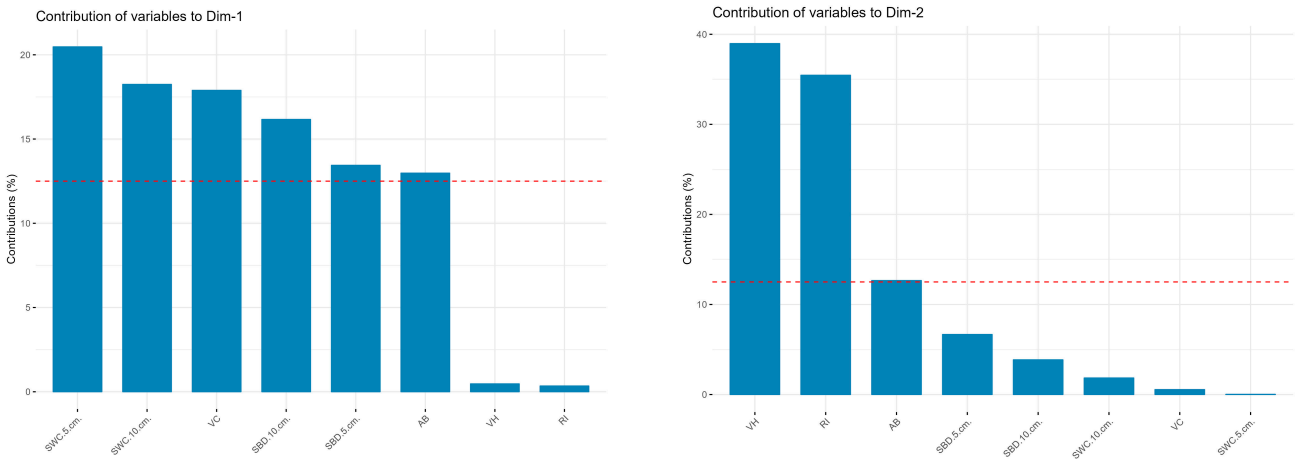

Figure 9. The contribution of different factors for the first PCA (**left**) and the second PCA (**right**).

However, there may be interactions or co-relationships between factors. We used the Pearson correlation analysis to explain these. From Table 4, we can see that the RC is significantly related to RI, and RI is significantly related to RV; their correlation coefficients reached 0.68 ($p < 0.05$) and 0.85 ($p < 0.01$), respectively. Meanwhile, VC is highly related to the 5 cm SWC layer, the 10 cm SWC, and the 5 cm SBD, and the correlation coefficients are 0.83 ($p < 0.01$), 0.76 ($p < 0.05$), and 0.69 ($p < 0.05$), respectively. There are also significant relationships between SWC and SBD, between VC and AB, and so on. Therefore, we need to explain the interactions between the factors that were observed to affect the runoff generation.

Table 4. The Pearson correlation between the different factors.

	RI	SWC 5 cm	SWC 10 cm	SBD 5 cm	SBD 10 cm	VC	VH	AB	RC	RV
RI	1									
SWC 5 cm	−0.138	1								
SWC 10 cm	0.05	0.909 **	1							
SBD 5 cm	0.054	0.899 **	0.918 **	1						
SBD 10 cm	0.052	0.933 **	0.886 **	0.910 **	1					
VC	−0.07	0.830 **	0.764 *	0.608	0.688 *	1				
VH	−0.058	−0.223	−0.263	−0.502	−0.395	0.265	1			
AB	−0.014	0.613	0.511	0.331	0.434	0.929 **	0.545	1		
RC	0.683 *	−0.299	−0.255	0.011	−0.15	−0.418	−0.427	−0.382	1	
RV	0.851 **	−0.25	−0.181	0.004	−0.079	−0.298	−0.311	−0.243	0.954 **	1

"*"—significantly related at the 0.05 level; "**"—significantly related at the 0.01 level.

3.4. Contributions of Factors Affecting Rainfall-Runoff Generation

SEM was used to analyze the relationship between rainfall-runoff and its influencing factors. The model includes four latent variables, RI, SWC, SBD, and vegetation (VE), and eight measurable variables: RI, SWC 0–5 cm (SWC.5 cm), SWC 5–10 cm (SWC.10 cm), SBD 0–5 cm (SBD.5 cm), SBD 5–10 cm (SBD.10 cm), VC, VH, and AB.

Through repeated fitting, evaluating, and correcting in the model, a final standardized coefficient model was constructed (Figure 10) and the GOF (goodness of fit) of the developed model achieved 0.66. And the Cronbach's alpha and DG.rho values are greater than 0.7 (Table 5), which indicates that the data have good consistency and can ensure the reliability of this study.

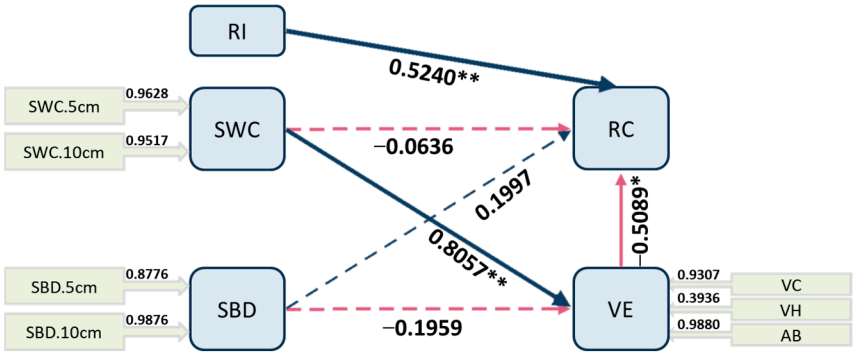

Figure 10. Mechanism of rainfall-runoff generation based on structural equation modelling (RI, RC, VE, SWC, and SBD represent the rainfall intensity, runoff coefficient, vegetation, soil water content, and soil bulk density, respectively; SWC.5 cm, SWC.10 cm, SBD.5 cm, and SBD.10 cm represent soil water content of 0–5 cm, soil water content of 5–10 cm, soil bulk density of 0–5 cm, and soil bulk density of 5–10 cm, respectively; VC, AB, and VH represent vegetation coverage, aboveground biomass, and vegetation height, respectively; "**" level of significance of $p < 0.01$; "*" level of significance of $p < 0.05$).

Table 5. Variables list and data reliability values.

Variables	Cronbach's Alpha	DG.rho
RI	1.00	1.00
SWC	0.91	0.96
SBD	0.84	0.93
VA	0.71	0.85
RC	1.00	1.00

The standardized path coefficient was used to measure the contribution of each factor to runoff generation. The value on the line represents the standardized path coefficient, indicating the influencing degree of the independent variable on the dependent variable. The positive or negative value of the standardized path coefficient indicates a positive or negative correlation. The arrows point from the independent variable to the dependent variable. From Figure 10, we can see that the factor that has the greatest direct positive significant ($p < 0.01$) impact on RC is RI, with a standardized path coefficient of 0.52. VE has a direct negative significant ($p < 0.05$) impact on RC with a standardized path coefficient of −0.51. However, SWC has no direct impact on RC, while SWC affects RC significantly by affecting vegetation condition. SWC has a great positive effect on VE, with a standardized path coefficient of 0.81 ($p < 0.01$). The SBD has no significant impact on RC. The contributions of the 5 cm SWC layer and the 10 cm SWC layer have a similar weight (0.96 and 0.95, respectively) on the vegetation condition. However, among the vegetation conditions, AB has greatest weight, with a coefficient of 0.99, followed by VC with 0.93; meanwhile, VH has smaller impact on RC, with a coefficient of only 0.39.

4. Discussion

Water resources redistribution (evaporation, plant interception, surface runoff, and soil infiltration) following a rainfall event comprise a major factor in hydrological processes. Hydrological regimes in small semi-arid watersheds have unique characteristics. However, studies of rainfall-runoff generation patterns in desert steppes are scarce, and their influencing factors remain unclear. This on-site rainfall-runoff simulation experiment revealed that rainfall-runoff generation is mostly driven by RI's coupling with the land degradation levels in a given desert steppe. The maximum runoff volumes in different degraded plots were found to differ significantly. Compared with the initial stage of runoff generation, as time progressed, the surface accumulation of runoff and the water flow velocity increased

due to a decrease in soil saturation and infiltration; then, the runoff volume increased to its peak after a period of time. Meanwhile, the peak value and the time taken to reach the peak value were found to be different in different plots. In general, the influencing factors of the rainfall-runoff generation include RI, initial soil water content, vegetation condition, soil texture, topography, and land management.

4.1. Reason of the Lower Runoff Coefficient

This study revealed that the RC in the chosen desert steppe did not exceed 0.4, which is lower than the published runoff coefficient at a regional scale.

The RC is the ratio of the total runoff (mm) to the precipitation (mm) in a certain watershed area during a given period of time. It is also the ratio of the runoff depth to the precipitation depth in any period of time corresponding to the runoff in that period. The RC is a comprehensive index reflecting the runoff characteristics in a given watershed. It represents how much of precipitated water becomes runoff. The value of RC varies between 0 and 1. A greater value indicates that there is a larger amount of runoff, and vice versa. This value is generally higher in humid areas and lower in arid areas. The RC of a given area is mainly affected by VC, AB, and soil characteristics (soil texture, SWC).

The RC in this study was calculated for the period between the start time of rainfall and the time taken to reach a maximum runoff level. The study site used in this experiment is a typical arid and semi-arid desert steppe region which experiences different levels of degradation. In such a region as that used in this study, rainfall reaches very low levels and precipitation occurs infrequently. Additionally, the amount of water in the river has been continuously decreasing in recent years. Therefore, the soil in this region is generally in a state of drought. In addition, the main soil texture is silty loam, which is characterized by strong permeability and poor water stability. Thus, most rainfall water may permeate into the soil and thus generate low levels of runoff.

In addition, the average 0–5 cm and 5–10 cm SBDs are 1.43 and 1.46, respectively. In general, SBD values are between 1 and 1.5. The looser and the more porous the soil in a given area, the smaller the SBD value is. This indicates that the compactness of the soil in this area is relatively high; therefore, this can be noted as another reason affecting the low RC value.

4.2. Influence of Soil Characteristic on Runoff Generation

Soil is the main link in the surface–groundwater interaction. It has been shown that the physical properties of soil, such as SBD, saturated hydraulic conductivity, soil porosity, and saturated SWC, also play important roles in the generation of rainfall-runoff [43–45].

We did not measure the soil texture through soil sampling or testing in this study. However, according to previous experiments, the soil texture of the soil at our experiment site is silty loam. Silt loam has moderate permeability and poor water stability. Therefore, when rainfall begins or RI is lower, most precipitation water permeates into the soil and thus no/less runoff is generated. However, when SWC is close to saturation, soil erosion occurs, further aggravating land degradation.

SWC and SBD are important soil parameters which interact with each other; these have a direct impact on soil water movement processes. Here, we measured the initial soil water content and SBD at the 0–5 cm, 5–10 cm, 10–15 cm, and 15–20 cm levels for the three different degradation levels. The details of these measurements are presented in Table 2.

SBD is an important indicator of soil quality, which reflects the porosity of soil. When clay content is higher, SBD is higher and porosity is lower, and vice versa. A larger SBD value indicates that the soil is more tightly packed and that it has lower porosity. In general, the SBD value of clay soil (1.0–1.5 g/cm^3) is lower than that of sandy soil (1.2–1.8 g/cm^3). And the SBD value is generally lower in soils with high organic matter contents and good structures. Thus, in our experiment, the SBD value is high due to the degraded nature of the studied desert steppe. During the hydrological cycle of evaporation, rainfall, infiltration, and runoff, surface soil undergoes a process where it transitions from dry to wet and then

from wet to dry. When the soil becomes wet, its water regime comes close to a status of saturated water content, and soil particles expand greatly and seal its pores. When soil becomes dry, the surface area will shrink, resulting in cracks and changing the structure of the soil; in this period, SBD values change accordingly.

The SWC values in the HD, MD, and LD plots were about 2.9, 5.0, and 4.0 in the 0–5 cm depth, respectively, and were 2.9, 4.8, and 3.8 in the soil depth of 5–10 cm, respectively, at the chosen experiment site. The SWC values in the different degraded plots and different soil layers differed to a certain degree. The results of the SEM suggest that SWC has an indirect impact on runoff generation through having an effect on the vegetation condition, while SBD was not found to have a significant impact on runoff generation. Therefore, we consider that the impact of SWC and the interaction between SWC and vegetation are complicit in the measured degradation levels and have a role in amplifying differences in the rainfall-runoff generation characteristics between different degradation levels.

Several studies [10,46–48] have demonstrated that there is a threshold in the relationship between SWC and runoff generation; when the SWC exceeds this threshold, the runoff increases sharply. However, the SWC threshold for runoff generation in the chosen desert steppe remains uncertain. Therefore, when designing the experiment, including the location and time, we consciously avoided the influence of soil moisture as much as possible.

4.3. Influence of Land Degradation on Runoff Coefficient in Desert Steppe

Land degradation encompasses the degradation of vegetation, soil, water, ecosystem service, etc. The findings of this study indicate that land degradation levels have a significant impact on rainfall-runoff generation. The RC value increases with the land degradation level, characterized by the following order: LD < MD < HD. This has been proven and indicated in a previous study, where the highest efficiency in controlling runoff was observed in a plot with a 100% canopy cover [48]. The RC value was negatively associated with vegetation conditions, which indicates that grass intercepts rain drops (reducing the velocity of runoff) and accelerates penetration (increases the infiltration rate), and then reduces runoff [49–51], thereby increasing soil water content and groundwater content. In addition, vegetation determines litter type, coverage, and soil humus, and further affects the characteristics of runoff generation in a given area [52]. This implies that the degradation of grassland induces a series of ecological and hydrological consequences, such as increased runoff, aggravated water and soil erosion, loss of soil nutrients, reduced soil water capacity, reduced grassland productivity, and increasingly severe drought (an important topic in climate change); consequently, such factors can bring about huge effects in the social–economic development of a given area, especially the livestock production in desert steppes.

4.4. Interactions among Multiple Factors Generating Runoff

It is extremely important to quantify the contribution of multiple influencing factors and to clarify the processes of the interactions among various factors. SEM can effectively integrate statistical factor analysis and path analysis and can describe the relationships between variables that cannot be directly measured. In this study, we developed an SEM to elucidate the interaction between the different influencing factors in the study area. We found that the generated final runoff was driven by interactions among multiple influencing factors. The SEM can only explain linear relationships between different factors; it cannot determine nonlinear relationships between influencing factors.

This study mainly reveals the rainfall-runoff generation characteristics and the factors influencing the rainfall-runoff generation in the chosen desert steppe. This is an important basis for explaining the hydrological responses of watersheds to land surface dynamics. However, runoff generation is affected by many factors, including climate, vegetation, soil, water, etc., which differ across different locations. Therefore, the result from a plot-scale experiment cannot fully elucidate watershed-scale or regional-scale phenomena. In addition, due to difficulties encountered during the rainfall simulation experiment, we only

considered the RI and vegetation conditions; the topographies and the ground-water were not accounted for. Thus, the plot-scale findings of this study cannot be directly generalized to the watershed scale.

In the future, we need to a develop robust model for investigating watershed- and regional-scale rainfall-runoff generation using remote sensing and GIS technology. The rapid progress of remote sensing products, GIS technology, artificial intelligence technology, and machine learning algorithms, in combination with the availability of remote sensing data on soil moisture, vegetation, water, land use, etc., offer a convenient opportunity to determine the characteristics of large-scale rainfall runoff generation.

5. Conclusions

Rainfall-runoff generation is a main factor impacting soil erosion and ecosystem degeneration. In order to determine and explore the characteristics of rainfall-runoff generation and its influencing factors in desert steppes, we carried out an artificial rainfall simulation experiment.

Rainfall-runoff was found to be generated faster and accumulated larger volumes under high RI (60 mm/h) in the HD plot in comparison with that under moderate/low RIs in the MD/LD plots. The accumulated runoff over 40 min under a high RI in the HD plot was found to be 153.37 L, which was much larger than that (0.77 L) from a low RI on the LD plot. The RC was found to be positively related to the RI value, and negatively related to VC and AB. An SEM indicated that RI is the most important direct positive influencing factor, with a standardized path coefficient of 0.52. VE was found to have a direct negative impact on runoff generation with a standardized path coefficient of −0.51. It is notable that SWC was found to have a significant indirect impact on runoff generation through affecting vegetation. Therefore, a larger range of changes in runoff generation characteristics (the starting time, the duration, and the volume) was induced by RI compared to the degradation levels. The influencing factors selected in our study were found to explain 74.7% of the total runoff generation. There are other factors that should be taken into consideration in the future. This study implies that we can reduce runoff generation through enhancing vegetation, altering soil properties, and optimizing their correlation.

Author Contributions: H.: data analysis, writing—original draft preparation, review, and editing. T.L.: investigation, data collection and data analysis. J.L.: suggestions for writing—review and editing. All authors have read and agreed to the published version of the manuscript.

Funding: This research was funded by the Open Research Fund of State Key Laboratory of Simulation and Regulation of Water Cycle in River Basin (China Institute of Water Resources and Hydropower Research), Grant NO: IWHR-SKL-202014, National Natural Science Foundation of China General Program (51779156), Natural Science Foundation of Inner Mongolia Autonomous Region-Major Project (2021ZD12) and the Program for Innovative Research Team in Universities of Inner Mongolia Autonomous Region (NMGIRT2313).

Institutional Review Board Statement: Not applicable.

Informed Consent Statement: Not applicable.

Data Availability Statement: The data are available upon request from the corresponding author.

Conflicts of Interest: The authors declare that they have no known competing financial interests or personal relationships that could have appeared to influence the work reported in this paper.

References

1. Rupak, S.; Subashisa, D.; Amit Kumar, D. An insight into the runoff generation processes in wet sub-tropics: Field evidences from a vegetated hillslope plot. *Catena* **2015**, *128*, 31–43.
2. Ran, Q.H.; Su, D.Y.; Li, P.; He, Z.G. Experimental study of the impact of rainfall characteristics on runoff generation and soil erosion. *J. Hydrol.* **2012**, *424*, 99–111. [CrossRef]

3. Dong, L.; Xiong, L.; Yu, K.; Li, S. Advances in the study of impacts of climate change and human activities on hydrology. *Adv. Water Sci.* **2012**, *23*, 278–285.
4. Tian, Y.; Zhang, M.; Xu, D.; Zhang, S. Construction of ecological security pattern of urban landscape based on the theory of 'source-sink'. *J. Ecol.* **2019**, *39*, 2311–2321.
5. Li, Y.F.; Luo, Y.C.; Liu, G.; Ouyang, Z.Y.; Zheng, H. Effects of land use change on ecosystem services: A case study of Miyun Reservoir Basin. *J. Ecol.* **2013**, *33*, 726–736.
6. Nurland, H.; Shen, Y.; Mahathir, M. Impact of climate change on runoff processes in the Urengu River Basin, Altai Mountains. *Glacier Permafr.* **2014**, *36*, 699–705.
7. Guzha, A.C.; Rufino, M.C.; Okoth, S.; Jacobs, S.; Nóbrega, R.L.B. Impacts of land use and land cover change on surface runoff, discharge and low flows: Evidence from East Africa. *J. Hydrol. Reg. Stud.* **2018**, *15*, 49–67. [CrossRef]
8. He, B.; Gao, F.; Tang, X.; Qin, S. Diagnosis of hydrometeorological variability of arid inland rivers in Xinjiang based on sliding Copula function. *Soil Water Conserv. Res.* **2019**, *26*, 155–161.
9. Liu, W.; Li, Z.; Zhu, J.; Xu, C.; Xu, X. Dominant factors controlling runoff coefficients in karst watersheds. *J. Hydrol.* **2020**, *590*, 125486. [CrossRef]
10. Xiao, X.; Zhang, F.; Che, T.; Shi, X.; Zeng, C.; Wang, G. Changes in plot-scale runoff generation processes from the spring–summer transition period to the summer months in a permafrost-dominated catchment. *J. Hydrol.* **2020**, *587*, 124966. [CrossRef]
11. Mügler, C.; Planchon, O.; Patin, J.; Weill, S.; Silvera, N.; Richard, P.; Mouche, E. Comparison of roughness models to simulate overland flow and tracer transport experiments under simulated rainfall at plot scale. *J. Ecol.* **2011**, *402*, 25–40. [CrossRef]
12. Garel, E.; Marc, V.; Ruy, S.; Cognard-Plancq, A.L.; Klotz, S.; Emblanch, C.; Simler, R. Large scale rainfall simulation to investigate infiltration processes in a small landslide under dry initial conditions: The Draix hillslope experiment. *Hydrol. Process.* **2012**, *26*, 2171–2186. [CrossRef]
13. Tromp-van Meerveld, H.; Seibert, J.; Peters, N. Hillslope-riparian-stream connectivity and flow directions at the Panola Mountain research watershed. *Hydrol. Process.* **2015**, *29*, 3556–3574. [CrossRef]
14. Rushlow, C.; Godsey, S. Rainfall-runoff responses on Arctic hillslopes underlain by continuous permafrost, North Slope, Alaska, USA. *Hydrol. Process.* **2017**, *31*, 4092–4106. [CrossRef]
15. Hu, G.; Li, X.; Yang, X. The impact of micro-topography on the interplay of critical zone architecture and hydrological processes at the hillslope scale: Integrated geophysical and hydrological experiments on the Qinghai-Tibet Plateau. *J. Hydrol.* **2020**, *583*, 124618. [CrossRef]
16. Sharma, R.D.; Sarkar, R.; Dutta, S. Run-off generation from fields with different land use and land covers under extreme storm events. *Curr. Sci.* **2013**, *104*, 1046–1053.
17. Deng, Z.M.; Zhang, X.; Li, D. Simulation of land use/land cover change and its effects on the hydrological characteristics of the upper reaches of the Hanjiang Basin. *Environ. Earth Sci.* **2015**, *73*, 1119–1132. [CrossRef]
18. Laughlin, D.C.; Laughlin, D.E. Advances in modeling trait-based plant community assembly. *Trends Plant Sci.* **2013**, *18*, 584–593. [CrossRef]
19. Hou, J.; Wang, H.Q.; Fu, B.J.; Zhu, L.H.; Wang, Y.F.; Li, Z.S. Effects of plant diversity on soil erosion for different vegetation patterns. *Catena* **2016**, *147*, 632–637. [CrossRef]
20. Fu, B.; Wang, S.; Liu, Y.; Liu, J.; Liang, W.; Miao, C. Hydrogeomorphic ecosystem responses to natural and anthropogenic changes in the loess plateau of China. *Annu. Rev. Earth Planet. Sci.* **2017**, *45*, 223–243. [CrossRef]
21. Yu, Y.; Wei, W.; Chen, L.; Feng, T.; Daryanto, S. Quantifying the effects of precipitation, vegetation, and land preparation techniques on runoff and soil erosion in a Loess watershed of China. *Sci. Total Environ.* **2019**, *652*, 755–764. [CrossRef] [PubMed]
22. Nasonova, O.N.; Gusev, Y.M.; Kovalev, Y.E. Impact of uncertainties in meteorological forcing data and land surface parameters on global estimates of terrestrial water balance components. *Hydrol. Process.* **2011**, *25*, 1074–1090. [CrossRef]
23. Boulange, J.; Malhat, F.; Jaikaew, P.; Nanko, K.; Watanabe, H. Portable rainfall simulator for plot-scale investigation of rainfall-runoff, and transport of sediment and pollutants. *Int. J. Sediment Res.* **2019**, *34*, 38–47. [CrossRef]
24. Iserloh, T.; Ries, J.B.; Cerdà, A.; Echeverría, M.T.; Fister, W.; Geiler, C.; Kuhn, N.J.; León, F.J.; Peters, P.; Schindewolf, M.; et al. Comparative measurements with seven rainfall simulators on uniform bare fallow land. *Z. Geomorphol.* **2013**, *57*, 11–26. [CrossRef]
25. Zhao, N.N.; Yu, F.L.; Li, C.Z.; Wang, H.; Liu, J.; Mu, W.B. Investigation of Rainfall-Runoff Processes and Soil Moisture Dynamics in Grassland Plots under Simulated Rainfall Conditions. *Water* **2014**, *6*, 2671–2689. [CrossRef]
26. Coles, A.E.; McDonnell, J.J. Fill and spill drives runoff connectivity over frozen ground. *J. Hydrol.* **2018**, *558*, 115–128. [CrossRef]
27. Jadidoleslam, N.; Mantilla, R.; Krajewski, W.F.; Goska, R. Investigating the role of antecedent SMAP satellite soil moisture, radar rainfall and MODIS vegetation on runoff production in an agricultural region. *J. Hydrol.* **2019**, *579*, 124210. [CrossRef]
28. Bretherton, M.; Horne, D.; Sumanasena, H.A.; Jeyakumar, P.; Scotter, D. Repellencyinduced runoff from New Zealand hill country under pasture: A plot study. *Agric. Water Manag.* **2018**, *201*, 83–90. [CrossRef]
29. Wilson, C.; Kampf, S.K.; Wagenbrenner, J.W.; MacDonald, L.H. Rainfall thresholds for post-fire runoff and sediment delivery from plot to watershed scales. *For. Ecol. Manag.* **2018**, *430*, 346–356. [CrossRef]
30. Zhang, N.; Luo, Y.-J.; Chen, X.-Y.; Li, Q.; Jing, Y.-C.; Wang, X.; Feng, C.-H. Understanding the effects of composition and configuration of land covers on surface runoff in a highly urbanized area. *Ecol. Eng.* **2018**, *125*, 11–25. [CrossRef]
31. Shi, P.; Zhang, Y.; Ren, Z.; Yu, Y.; Li, P.; Gong, J. Land-use changes and check dams reducing runoff and sediment yield on the Loess Plateau of China. *Sci. Total Environ.* **2019**, *664*, 984–994. [CrossRef]

32. Tian, W.; Liu, X.; Liu, C.; Bai, P. Investigation and simulations of changes in the relationship of precipitation-runoff in drought years. *J. Hydrol.* **2018**, *565*, 95–105. [CrossRef]
33. Xu, G.; Zhang, J.; Li, P.; Li, Z.; Lu, K.; Wang, X.; Wang, F.; Cheng, Y.; Wang, B. Vegetation restoration projects and their influence on runoff and sediment in China. *Ecol. Indic.* **2018**, *95*, 233–241. [CrossRef]
34. *GB+19377-2003*; Parameters for Degradation, Sandification and Salification of Rangelands. Chinese Standard: Beijing, China, 2003.
35. Crow, W.T.; Chen, F.; Reichle, R.H.; Xia, Y. Diagnosing bias in modeled soil moisture/runoff coefficient correlation using the SMAP Level 4 soil moisture product. *Water Resour. Res.* **2019**, *55*, 7010–7026. [CrossRef]
36. Jahanshahia, A.; Martijn, J.B. Exploring controls on rainfall–runoff events: Spatial dynamics of event runoff coefficients in Iran. *Hydrol. Sci. J.* **2023**, *68*, 954–966. [CrossRef]
37. Zhang, Z.; Chen, X.; Huang, Y.; Zhang, Y. Effect of catchment properties on runoff coefficient in a karst area of southwest China. *Hydrol. Process.* **2014**, *28*, 3691–3702. [CrossRef]
38. Yao, L.; Wei, W.; Chen, L.D. How does imperviousness impact the urban rainfall-runoff process under various storm cases? *Ecol. Indic.* **2016**, *60*, 893–905. [CrossRef]
39. Pan, T.; Hou, S.; Wu, S.; Liu, Y.; Liu, Y.; Zou, X.; Herzberger, A.; Liu, J. Variation of soil hydraulic properties with alpine grassland degradation in the eastern Tibetan Plateau. *Hydrol. Earth Syst. Sci.* **2017**, *21*, 2249–2261. [CrossRef]
40. Guiden, P.W.; Barber, N.A.; Blackburn, R.; Farrell, A.; Fliginger, J.; Hosler, S.C.; King, R.B.; Nelson, M.; Rowland, E.G.; Savage, K.; et al. Effects of management outweigh effects of plant diversity on restored animal communities in tallgrass prairies. *Proc. Natl. Acad. Sci. USA* **2021**, *118*, e2015421118. [CrossRef]
41. Tietje, M.; Antonelli, A.; Baker, W.J.; Govaerts, R.; Smith, S.A.; Eiserhardt, W.L. Global variation in diversification rate and species richness are unlinked in plants. *Proc. Natl. Acad. Sci. USA* **2022**, *119*, e2120662119. [CrossRef]
42. Zhang, M.; Wu, M. Analysis on the Mechanism and Transmission Path of the Impact of Land Use on Carbon Emissions: Empirical Test Based on Structural Equation Model. *China Land Sci.* **2022**, *3*, 96–103.
43. Spence, C. A paradigm shift in hydrology: Storage thresholds across scales influence catchment runoff generation. *Geogr. Compass* **2010**, *4*, 819–833. [CrossRef]
44. Penna, D.; Tromp-van Meerveld, H.J.; Gobbi, A.; Borga, M.; Dalla Fontana, G. The influence of soil moisture on threshold runoff generation processes in an alpine headwater catchment. *Hydrol. Earth Syst. Sci.* **2011**, *15*, 689–702. [CrossRef]
45. Tarasova, L.; Basso, S.; Zink, M.; Merz, R. Exploring controls on rainfall-runoff events: 1. Time series-based event separation and temporal dynamics of event runoff response in Germany. *Water Resour. Res.* **2018**, *54*, 7711–7732. [CrossRef]
46. Radatz, T.; Thompson, A.; Madison, F. Soil moisture and rainfall intensity thresholds for runoff generation in southwestern Wisconsin agricultural watersheds. *Hydrol. Process.* **2013**, *27*, 3521–3534. [CrossRef]
47. Farrick, K.; Branfireun, B. Soil water storage, rainfall and runoff relationships in a tropical dry forest catchment. *Water Resour. Res.* **2014**, *50*, 9236–9250. [CrossRef]
48. Ali, G.; Tetzlaff, D.; McDonnell, J. Comparison of threshold hydrologic response across northern catchments. *Hydrol. Process.* **2015**, *29*, 3575–3591. [CrossRef]
49. Gholami, V.; Sahour, H. Simulation of rainfall-runoff process using an artificial neural network (ANN) and field plots data. *Theor. Appl. Climatol.* **2022**, *147*, 87–98. [CrossRef]
50. El Kateb, H.; Zhang, H.; Zhang, P.; Mosandl, R. Soil erosion and surface runoff on different vegetation covers and slope gradients: A field experiment in Southern Shaanxi Province, China. *Catena* **2013**, *105*, 1–10. [CrossRef]
51. Han, D.D.; Deng, J.C.; Gu, C.J.; Mu, X.M.; Gao, P.; Gao, J.J. Effect of shrub-grass vegetation coverage and slope gradient on runoff and sediment yield under simulated rainfall. *Int. J. Sediment Res.* **2021**, *36*, 29–37. [CrossRef]
52. Gholami, V.; Sahour, H.; Khaleghi, M.R.; Yousefi, A. Evaluating the effects of vegetation and land management on runoff control using field plots and machine learning models. *Environ. Sci. Pollut. Res.* **2022**, *30*, 31202–31217. [CrossRef]

Disclaimer/Publisher's Note: The statements, opinions and data contained in all publications are solely those of the individual author(s) and contributor(s) and not of MDPI and/or the editor(s). MDPI and/or the editor(s) disclaim responsibility for any injury to people or property resulting from any ideas, methods, instructions or products referred to in the content.